Penerbit Akademia Baru

Journal of Advanced Research in Applied Mechanics

Journal homepage: www.akademiabaru.com/aram.html
ISSN: 2289-7895

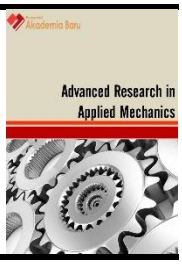

Analyzes of Flow Field Near the Combustor Endwall Surface Under the Usage of Row Trenched Cooling Holes

Open Access

Ehsan Kianpour[1], Nor Azwadi Che Sidik[1,*] Iman Golshokouh[2]

[1] Universiti Teknologi Malaysia, Jalan Sultan Yahya Petra, Kampung Datuk Keramat, 54100 Kuala Lumpur, Malaysia
[2] Faculty of Mechanical Engineering, Islamic Azad University of Izeh Branch, Izeh, Khuzestan, Iran

ARTICLE INFO

Article history:
Received 1 January 2019
Received in revised form 22 May 2019
Accepted 25 June 2019
Available online 21 November 2019

ABSTRACT

This study was done in order to investigate the effects of using row trenched cooling holes with an alignment angle of 0 and 90 degrees on the dynamic behavior of flow near the combustor end wall surface. Higher gas turbine engine efficiency is an important issue. Bryton cycle is a key to this. According to this cycle, it is required to increase the outlet combustion temperature. But this temperature increase creates harsh environment at the end of combustor and threatened the life of critical parts. So, the design of a cooling scheme is essential. Cooling is divided into two different parts –internal and external cooling- and film cooling is the common way which is seen in the external cooling. Film cooling effectiveness increment is achieved by coolant blowing ratio increase. However, with mass flux ratio augmentation, coolant not attach well on the protected surface. To solve the problem, it is needed to restructure the cooling holes. Trenching holes is a usual way. But the effects of trenched cooling holes at the end of combustor and the alignment angle of row trenched cooling holes are not considered yet. In this study a three dimensional presentation of true Pratt and Whitney gas turbine engine was simulated and analyzed with a commercial finite volume package FLUENT 6.2.26 for gathering the fundamental data. This combustor simulator combined the interaction of two rows of dilution jets, which staggered in the stream wise direction and aligned in the span wise direction. The entire findings of the study showed that with trenching cooling holes the turbulence level increased slowly from first cooling panel to the last one. At the leading edge of the jet, the jet mainstream interaction intensified the gradients of velocity especially for the trenched case.

Keywords:
Gas Turbine, Film-Cooling, Cylindrical Hole, Trenched hole, Dilution Jets

1. Introduction

Modern gas turbine industries try for higher engine efficiencies. Bryton cycle is a key to this achievement. According to this cycle, the turbine inlet temperature should increase to gain higher efficiency. However, the turbine inlet temperature increment creates an extremely harsh environment for critical downstream components such as turbine vanes. Therefore, it is required to

* *Corresponding author.*
E-mail address: azwadi@utm.my (Nor Azwadi Che Sidik)

design a cooling technique in this area. Film cooling is the traditional way which is used. In this system, a thin thermal boundary layer such as buffer zone is formed by cooling holes and attached on the protected surface. Cylindrical and trenched cooling holes are two schemes of these holes. However, to get a better film cooling effectiveness, it is needed to augment blowing ratio. According to the importance of this research, a broad literature search was conducted to collect the information.

Kianpour *et al*. [1,2] simulated the combustor endwall cooling holes with two different layouts and exit section are ratios. The results declared that while, the central part of the jets stayed nominally at the same temperature level for both configurations, the temperatures adjacent the wall and between the jets was a while cooler with less cooling holes.

Ethridge *et al*. [3] experimentally studied the film cooling effectiveness on the suction surface of first stage turbine vane. The results showed that at low blowing ratios, increasing turbulence level has no significant effect on film cooling, however, at high blowing ratios, the coolant not attached well on the protected surface and thereby film cooling effectiveness reduction occurred. These results rejected the Sarkar and Bose [4].

Hale *et al*. [5] measured the effectiveness of surface adiabatic film cooling adjacent to the cooling holes. They noted a variety of L/D ratios, injection angles as well as co-flow and counter-flow plenum feed configurations. The findings of their studies were compatible with Burd and Simon [6] results which reported that short injection holes enhanced film cooling and created a larger cold area downstream of the cooling holes.

Colban *et al*. [7,8] took measurements on a two-passage cascades to investigate the hole injection film cooling effectiveness. According to Peng and Jiang [9] findings, it is debated that the fan-shaped holes raised the film cooling effectiveness. Furthermore, Lutum *et al*. [10] and Gao *et al*. [11] stated that by 75 percent film cooling performance is found for the shaped holes at higher blowing ratios compared to cylindrical cases.

Yiping *et al*. [12] tested the effects of depth and width of trenches on the film cooling under overall cooling effectiveness of φ=0.6 as determined by Maikell *et al*. [13]. This constant value of overall cooling effectiveness declared that at the leading edge, the thermal barrier coating has moderate dependency to the stagnation line variation. Also it is figured out that the third (w=2.0D and d=0.75D) and fourth (w=3.0D and d=0.75D) case were more effective than other cases and base line case and it means the trench depth of 0.75D was the optimum one as well as approved by CFD studies.

Sundaram and Thole [14] and Lawson and Thole [15] studied the effects of trenched depth and width on film cooling performance at the vane-end Wall. The results showed that the maximum cooling effectiveness is obtained at the trench depth of 0.80D. However, Lawson and Thole stated that the trench depth of 0.8D has negative effect on the cooling performance downstream the cooling hole.

Stitzel and Thole [16] indicated that dilution jet injection is the dominant feature at the combustor exit, while with no dilution, the exit profile was relatively uniform with a high temperature and low total pressure flow in the mainstream. Furthermore, Scrittore [17] mentioned that increasing the dilution jet velocity adversely effects the surface cooling performance downstream of dilution jets.

However, up to now, investigation into the effects of trenching the cooling holes near the combustor end wall surface on the dynamic behavior of film cooling have not been carried out. There are several unanswered questions: How trenched cooling holes affect the dynamic behavior of film cooling performance at the combustor end wall compared to the cylindrical holes? Therefore, the purpose of the current study was to study the effects of row trenched cooling holes on film cooling dynamic behavior near the end wall combustor simulator. Also in order to measure the validity of

the results, a comparison between the data gained from this study and Stitzel and Thole [16] project was carried out.

2. Methods and Materials

In this study a three-dimensional representation of a true Pratt and Whitney gas turbine engine was simulated and analyzed to gain fundamental data. The schematic view of the combustor is shown in Figure 1. The final combustor simulator design width and inlet height was 111.8 cm and 99.1 cm respectively. The length of the combustor was 156.9 cm and the contraction angle was 15.8 degree. The contraction angle began at X=79.8 cm. The inlet cross sectional area was 1.11 square meters and the exit cross sectional area was reduced to 0.62 square meters. The combustor simulator included four film-cooled stream wise panels. The starting point of these panels was approximately at 1.6 m upstream of the turbine vanes. The first and second panels were 39.2 and 40.6 cm in length. The length of the next two panels was 36.8 cm and 43.2 cm. The low thermal conductivity of combustor panels were 1.27 cm in thickness allowed for adiabatic surface temperature measurements. Two different rows of dilution holes were considered within the second and third panels. These dilution rows were located at 0.67 m and 0.90 m downstream of the beginning of the combustor liner panels. The diameter of the first row and second row of dilution holes was 8.5 cm and 11.9 cm respectively.

The centerline of the second row was staggered with respect to those of the first row. In the current research, the combustor simulator involved three configurations of cooling holes. For the purpose of verification, the first arrangement (baseline or case 1) was designed similar to the Stitzel and Thole [16] In both cases, the film cooling holes were placed in equilateral triangles. The diameter of the film cooling holes was 0.76 cm and drilled at an angle of 30 degree from the horizontal surface. The length of each film cooling holes in the first model (baseline) was 2.5 cm. For the second and third cases are shown in Figure 2, the cooling holes placed within a row trench with alignment angle of 0 degree (case 2) and 90 degree (case 3). Furthermore, the trench depth and width was 0.75D and 1.0D respectively. A global coordinate system (X, Y and Z) was also selected.

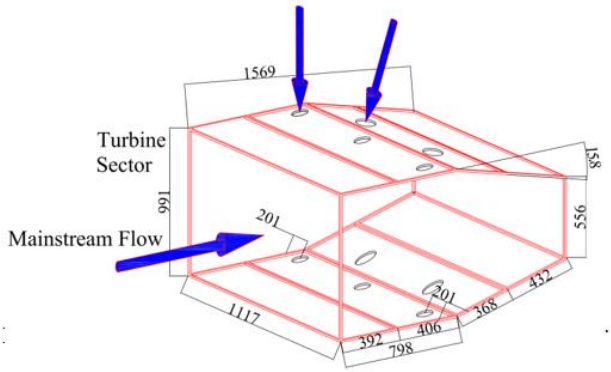

Fig. 1. 3-D view of the combustor simulator

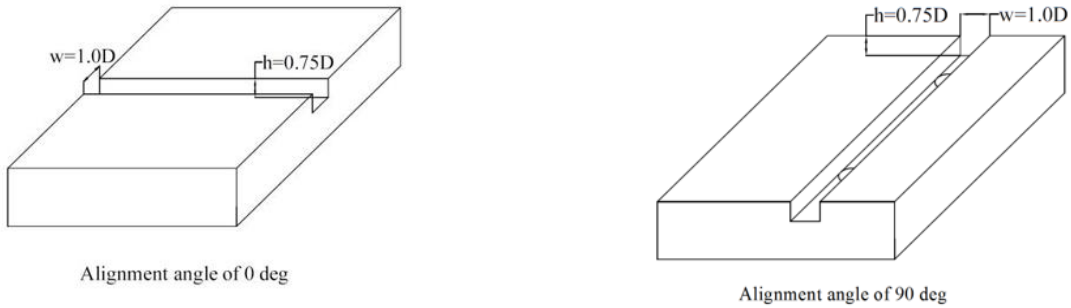

Fig. 2. Arrangement of trenched cooling holes with different alignment angles

The film cooling dynamic behavior in the combustor simulator was measured along the specific measurement planes. These measurement planes are illustrated in Figure 3a (baseline) 3b (case 2) and 3c (case 3). The flow field measurement planes of 0p, 1p, 2p and 3p were located in pitch wise direction and the measurement plane of 0s was placed in the stream wise direction. Plane 0p was placed exactly downstream of the first panel of cooling holes and at X=35.1 cm. The momentum distribution of film cooling is determined along this panel. This measurement plane covered half of the combustor simulator in the span wise direction. The height of the measurement plane covered 0cm<Z<10cm.

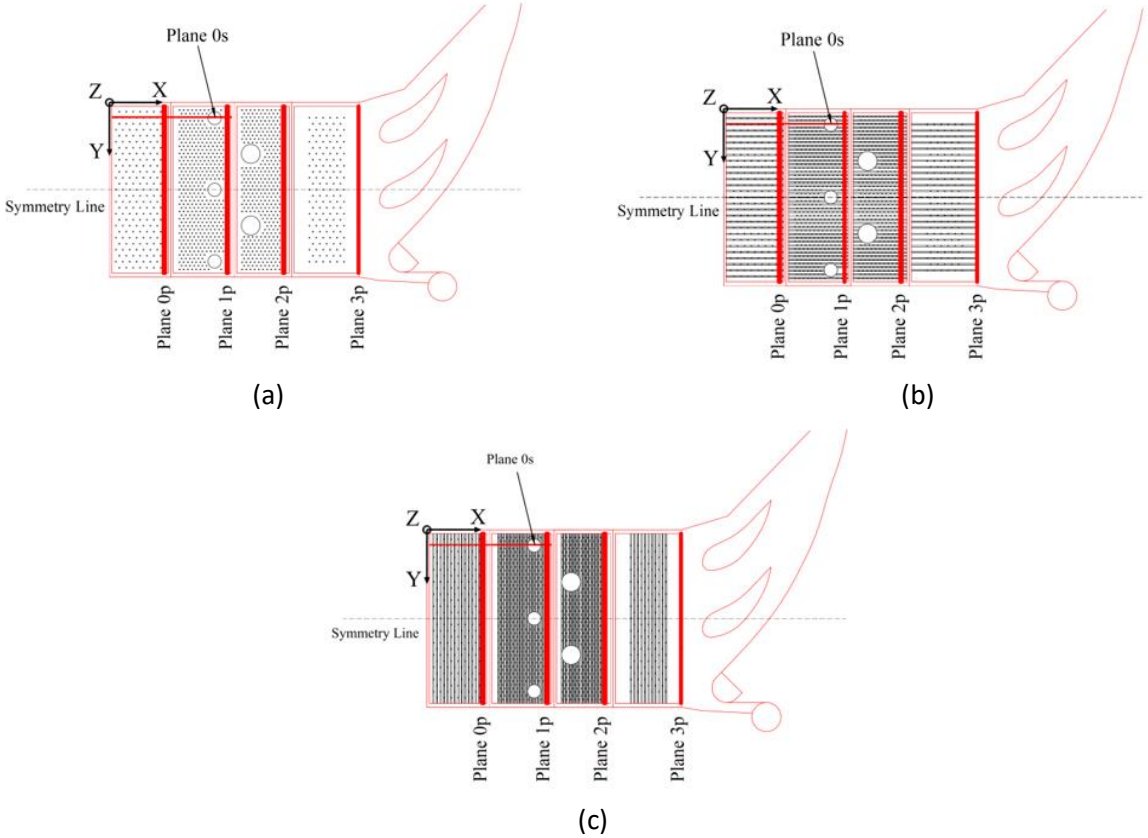

Fig. 3. Location of the measurement planes (a) baseline (b) Case 2(c) case 3

Plane 1p was located downstream of the first row of dilution jet at X=74.85cm. This plane was extended from Z=0cm to Z=10cm and covered the half width of the combustor simulator. This plane was used to measure the effects of film cooling on the dilution flow. This plane was also used to determine the effects of horseshoe, half-wake and counter rotating vortexes. Plane 2p was located

downstream of the trailing edge of the second row of dilution holes. This plane was placed at X=1.1cm and was extended along the vertical axis from Z=0.09cm to 0.22cm. The intent of this plane was to characterize the downstream interaction of the first and second rows of dilution on film cooling. Plane 3p was set at the end of combustor simulator. This plane was used to study the film cooling flow behavior section. Plane 0s was located directly at the central point of first row of dilution jet at Y=9.3cm and covered from X=39.2cm to X=78.45cm. This plane was used to study the interaction of flow along the first row of dilution jets.

In order to solve the combustor simulator problem and to get more precise data in a reasonable time, about 8×10^6 tetrahedral meshes were required. As demonstrated in Figure 4, the meshes were denser around the cooling and dilution holes as well as wall surfaces.

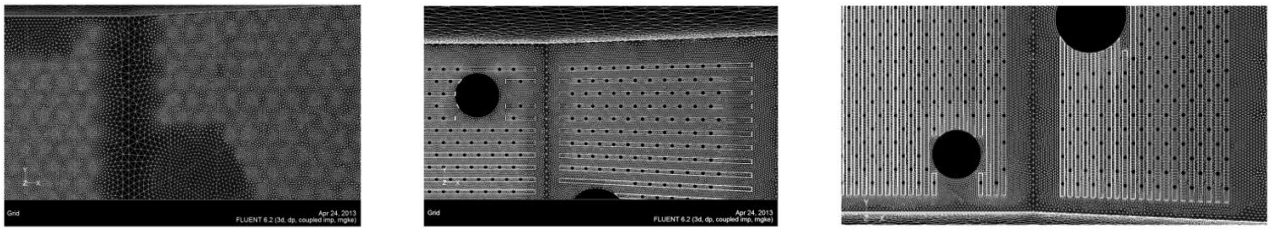

(a) (b) (c)

Fig. 4. Three dimensional meshes of combustor simulator (a) baseline (b) case 2 (c) case 3

This number of elements allows adequate convergence for refined meshing; the flow characters would have the same variation as the higher refinement mesh. The accuracy of the number of meshes used in this study was in concurrence with an investigation by Stitzel and Thole [16].

According to the specific flow rate at the volume control inlet, inlet mass flow boundary condition was defined at the inlet. Wall boundary condition and slip less boundary condition were applied to limit the interaction zone between fluid and solid layer. Furthermore to compare the findings of the current study with the previous results as reported [16,i], the inlet flow boundary was set as uniform flow and pressure outlet at the exit. Finally, according to the symmetries of the Pratt and Whitney engine combustor, symmetry boundary condition $\frac{\partial}{\partial n} = 0$ was applied.

The combustor simulator was meshed by Gambit software and the collected data were simulated and analyzed by using Fluent 6.2.26 software. The corresponding results were presented in the form of charts and different contours. In order to test the validity of the computational findings, the results will be crosschecked with the findings which obtained from Stitzel and Thole [16] researches. The numerical method considered a transient, incompressible turbulent flow by means of the RNG k-ε turbulent model of the Navier-Stokes equations expressed as follows:

Continuity equation:

$$\frac{\partial \rho}{\partial t} + \frac{\partial}{\partial x}\frac{dx}{dt} + \frac{\partial \rho}{\partial y}\frac{dy}{dt} + \frac{\partial \rho}{\partial z}\frac{dz}{dt} = -\rho(\nabla . V) \quad (1)$$

Momentum equation:

$$\frac{\partial}{\partial t}(\rho u_i) + \frac{\partial}{\partial x_i} = (\rho u_i u_j) = -\frac{\partial P}{\partial x_i} + \frac{\partial \tau_{ij}}{\partial x_i} + \rho g_i + \vec{F}_i \quad (2)$$

Energy equation:

$$\frac{\partial}{\partial t}(\rho E) + \frac{\partial}{\partial x_i}\left(u_i(\rho E + P)\right) = \frac{\partial}{\partial x_i}\left(k_{eff}\frac{\partial T}{\partial x_i} - \sum_j h_j J_j + u_j(\tau_{ij})_{erf}\right) + S_h \quad (3)$$

and RNG K-ε equation:

$$\frac{\partial}{\partial t}(\rho K)+\frac{\partial}{\partial x_i}(\rho K u_i)=\frac{\partial}{\partial x_j}\left[\left(\mu+\frac{\mu_t}{\sigma_K}\right)\frac{\partial K}{\partial x_j}\right]+P_K-\rho\epsilon \quad (4)$$

$$\frac{\partial}{\partial t}(\rho\epsilon)+\frac{\partial}{\partial x_i}(\rho\epsilon u_i)=\frac{\partial}{\partial x_j}\left[\left(\mu+\frac{\mu_t}{\sigma_\epsilon}\right)\frac{\partial \epsilon}{\partial x_j}\right]+C_{1\epsilon}\frac{\epsilon}{K}P_K-C_{2\epsilon}^{*}\rho\frac{\epsilon^2}{K} \quad (5)$$

To understand the thermal field results, the quantities should be defined. The velocity in the X, Y and Z direction is shown by *u*, *v* and *w*. These velocities are non-dimensionalized by the velocity of mainstream (u_{in}).

3. Results and Discussions

Figure 5 shows a comparison of u/u_{in} contour and v/u_{in} and w/u_{in} vectors for the current study and the computational findings of Stitzel for the baseline case. From both contours, it is found that behind the dilution jet, the flow is entrained significantly. As a result, a notable part of flow is entrined to the left side and this in concurred with Stitzel data. The being of three principal vortices in computational findings was the obvious difference between these results. These vortices were the rests of the first row of dilution jets with the mainstream and second row of dilution jets interaction.

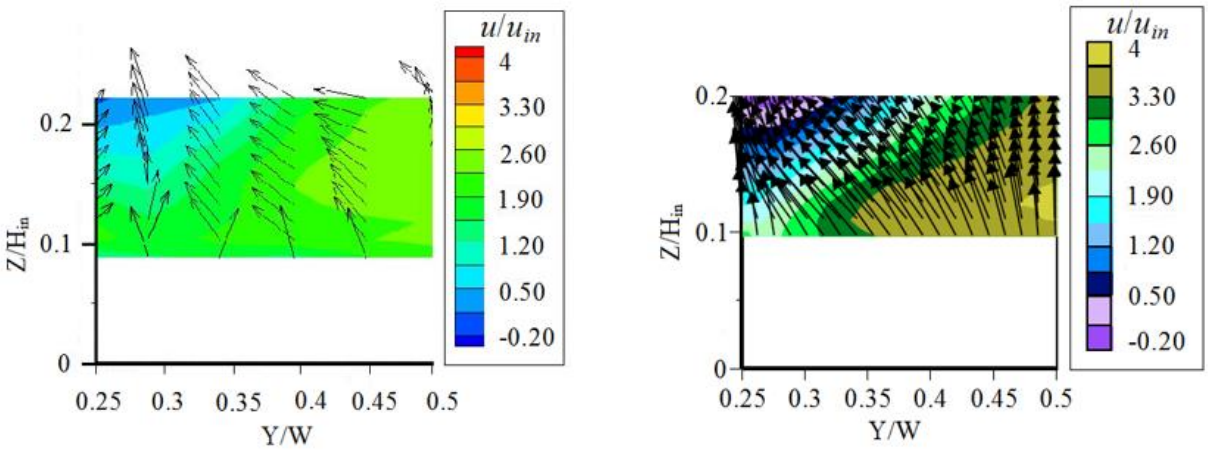

Fig. 5. Comparison of u/u_{in} contours and v/u_{in} and w/u_{in} vectors of plane 2p

The comparison was made for baseline case among the numerical results by Stitzel and Thole [16] and the current study. Figure 6 shows the comparison of velocity changes adjacent the end wall surface for plane 2p at Y/W=0. The deviations between the current computation and benchmarks were calculated as follows:

$$\%Diff=\frac{\sum_{i=1}^{n}\frac{x_i-x_{i,benchmark}}{x_{i,benchmark}}}{n} \quad (7)$$

According to this equation, the deviation was equal to 12.58%.

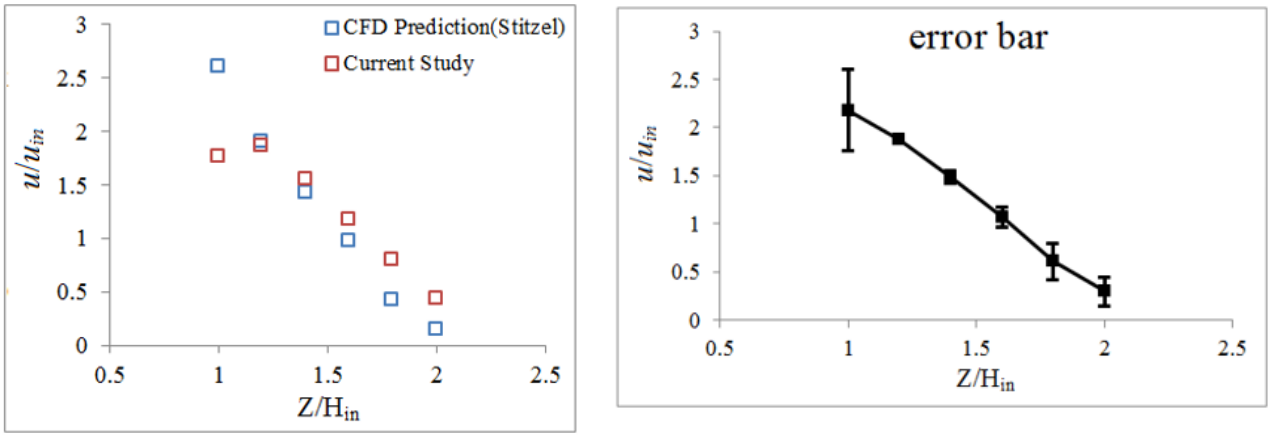

Fig. 6. Plots of stream wise velocity for plane 2p along Y/W = 0

Figure 7 shows the stream wise velocity contour and the cross-span velocity vectors of plane 0p. This figure declared that with the application of trenched holes the reversed flow was intensified near the end wall surface and this issue showed that the coolant not injected to the further area and attached on the protected surface. In addition, for this measurement plane, the flow changes were not dominant and it was almost equal to the velocity of mainstream.

Figure 8 shows the stream wise velocity contour and cross-span velocity vectors of v/u_{in} and w/u_{in} for plane 1p. The most immediate feature of this figure is the clock wise and counter-clock wise rotating vortexes, seen at the left and right side of the contour. The existence of in-line opposing rows of dilution jets forced the centers of counter rotating vortexes to spread further apart. On the upper section, the higher stream vise velocities are apparent and these velocities are intensified for trenched cases, especially for the trenched hole with alignment angle of 90 degree. However, it is seen that near the end wall surface, the stream wise velocity component was negative and this is indicated the being of reverse flow in the recirculating region just downstream of the jet.

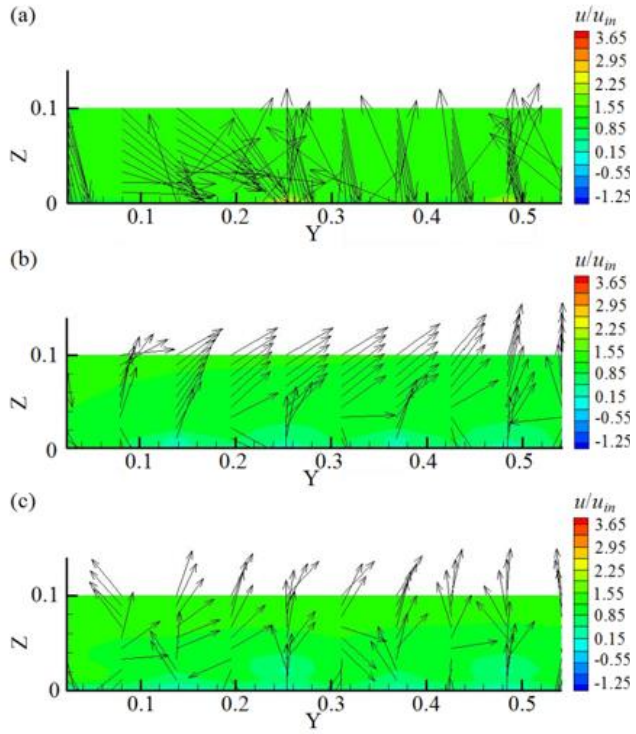

Fig. 7. Three-component velocity measurements for plane 0p (a) baseline (b) Case 2 (c) case 3

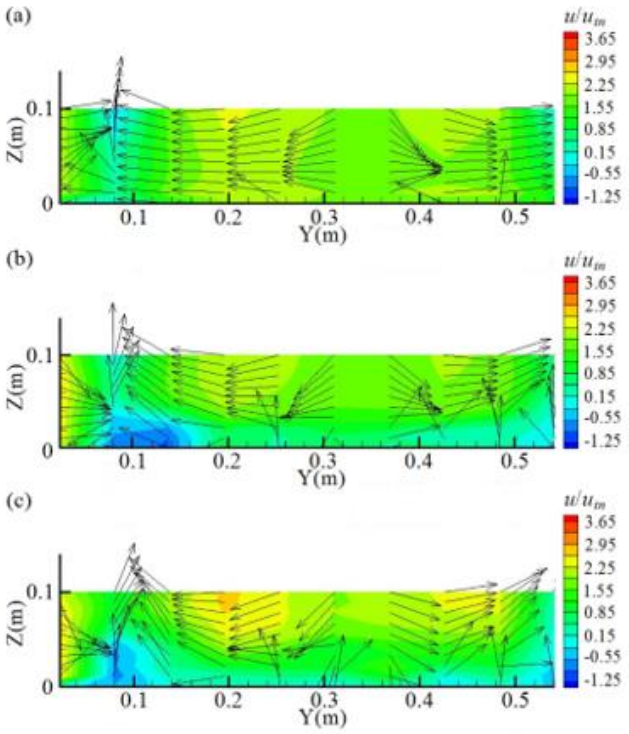

Fig. 8. Three-component velocity measurements of plane 1p (a) baseline (b) Case 2 (c) case 3

Figure 9 illustrates the three component velocity measurements for plane 2p: in particular contour of u/u_{in} and cross-span vectors of v/u_{in} and w/u_{in}. Surprisingly, the results were hard similar to the contour of plane 1p. The main difference was direction of the vortexes were completely different. The v/u_{in} and w/u_{in} velocity vectors show an intense upward flow adjacent the combustor end wall because of the contraction within the combustor. However, the velocity vectors were more turbulent for the trenched cases due to the interaction of the coolant injected from trenched holes and the main flow as a result of dilution jets. High turbulence levels can be seen on both sides of contours, however, it was most elevated for the trenched cases that the high turbulent level caused to remarkable reduction in the swirl velocities.

Figure 10 shows the flow field vectors of plane 0s from X=0.39m to X=0.78m. It was found that the flow was entrained to the upper level behind the dilution jet and the flow was accelerated within the combustor particularly for the trenched cases. The results declared that the downward motion of the leading edge of dilution jet, which was probably the result of the mainstream flow being deflected under the stagnation region. Downstream the dilution jet, the trenched holes not let the coolant injected to the further area.

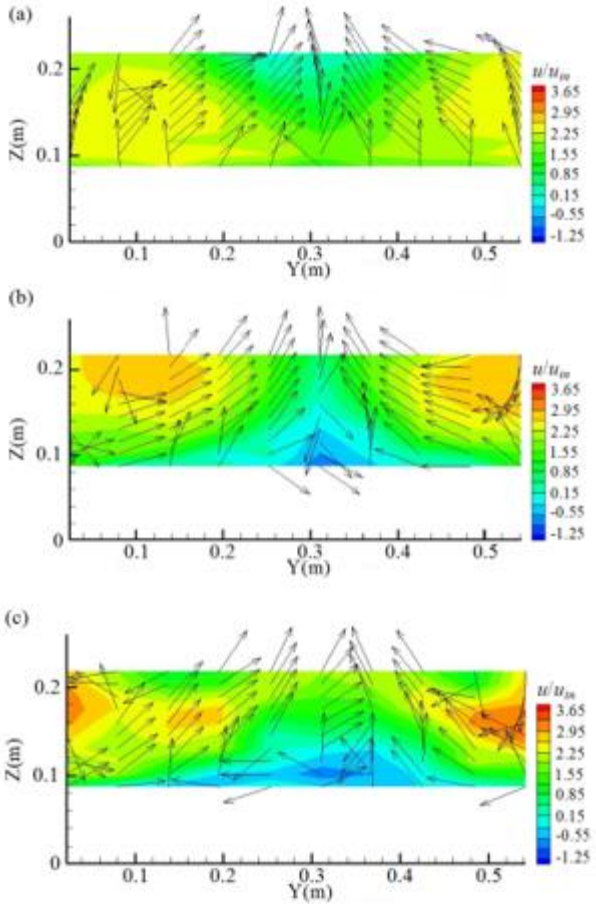

Fig. 9. The component velocity measurements for plane 2p (a) baseline (b) Case 2 (c) case 3

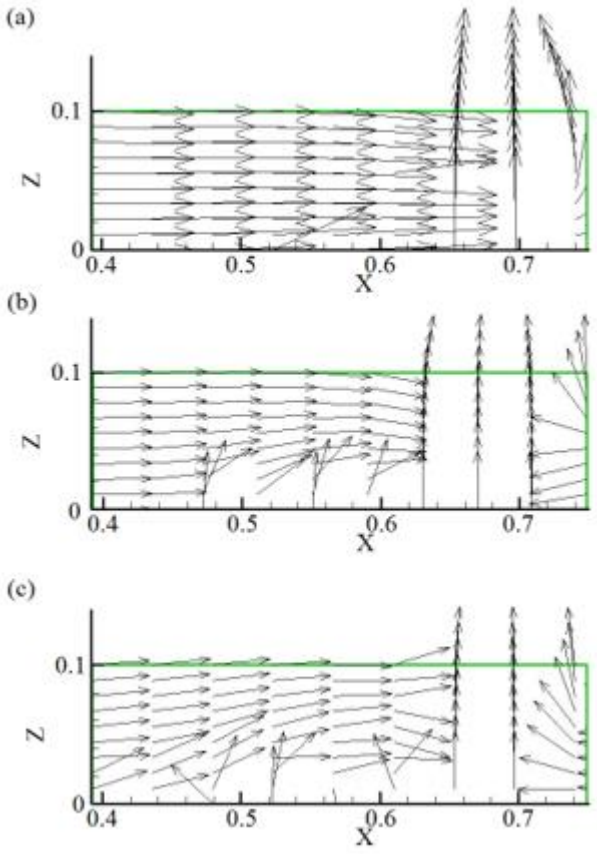

Fig. 10. Vectors of u/u_{in} and w/u_{in} for plane 0s (a) baseline (b) Case 2 (c) case 3

4. Conclusion

The purposes of this study were extending the database knowledge about the effects of different cooling holes' configurations of cylindrical and row trenched holes with alignment angle of 0 degree

and 90 degree at BR=3.18 on the dynamic behavior of film cooling at the end of combustor simulator. In this research, a three dimensional representation of a Pratt and Whitney gas turbine engine was simulated and analyzed to collect data. To sum up, due to the remnant of the upstream row of film cooling jets that exited from the aligned cooling holes the secondary flow was created and it was elevated by the trenched holes. The interaction between the in-line opposing dilution jets and the mainstream produced the shear layer that caused to the counter rotating vortexes pair. Near the end wall surface, the reverse flow was intensified from plane 0p to the last measurement plane particularly for the trenched arrangements. Between the current findings and Stitzel computational results there is a reasonable similarity which shows the entrainment of flow behind the dilution jet. In the future, different configurations of trenched cooling holes and baseline case should be considered for different cooling panels. Different cooling holes' arrangements affect the film cooling effectiveness at different cooling panels. The effects of different blowing ratios on the film cooling performance should be noticed as well.

References

[1] Kianpour, Ehsan, Nor Azwadi Che Sidik, and Mohsen Agha Seyyed Mirza Bozorg. "Thermodynamic analysis of flow field at the end of combustor simulator." *International Journal of Heat and Mass Transfer* 61 (2013): 389-396.

[2] Kianpour, E., Nor Azwadi Che Sidik, and Mohsen Agha Seyyed Mirza Bozorg. "Dynamic analysis of flow field at the end of combustor simulator." *Jurnal Teknologi* 58, no. 2 (2012).

[3] Ethridge, Marcia I., J. Michael Cutbirth, and David G. Bogard. "Scaling of performance for varying density ratio coolants on an airfoil with strong curvature and pressure gradient effects." *J. Turbomach.* 123, no. 2 (2000): 231-237.

[4] Sarkar, S., and T. K. Bose. "Numerical simulation of a 2-D jet-crossflow interaction related to film cooling applications: Effects of blowing rate, injection angle and free-stream turbulence." *Sadhana* 20, no. 6 (1995): 915-935.

[5] Hale, C. A., Michael W. Plesniak, and Satis Ramadhyani. "Film cooling effectiveness for short film cooling holes fed by a narrow plenum." *J. Turbomach.* 122, no. 3 (1999): 553-557.

[6] Burd, Steven W., and Terrence W. Simon. "Measurements of discharge coefficients in film cooling." (1999): 243-248.

[7] Colban, W., Karen Ann Thole, and M. Haendler. "A comparison of cylindrical and fan-shaped film-cooling holes on a vane endwall at low and high freestream turbulence levels." *Journal of Turbomachinery* 130, no. 3 (2008).

[8] Colban, W., A. Gratton, K. A. Thole, and M. Haendler. "Heat transfer and film-cooling measurements on a stator vane with fan-shaped cooling holes." *Journal of Turbomachinery* 128, no. 1 (2006): 53-61.

[9] Peng, W., and P-X. Jiang. "Experimental and numerical study of film cooling with internal coolant cross-flow effects." *Experimental Heat Transfer* 25, no. 4 (2012): 282-300.

[10] Lutum, E., J. Von Wolfersdorf, K. Semmler, S. Naik, and B. Weigand. "Film cooling on a convex surface: influence of external pressure gradient and Mach number on film cooling performance." *Heat and Mass Transfer* 38, no. 1-2 (2001): 7-16.

[11] Gao, Zhihong, Diganta Narzary, and Je-Chin Han. "Turbine blade platform film cooling with typical stator-rotor purge flow and discrete-hole film cooling." *Journal of Turbomachinery* 131, no. 4 (2009): 041004.

[12] Lu, Yiping, Alok Dhungel, Srinath V. Ekkad, and Ronald S. Bunker. "Effect of trench width and depth on film cooling from cylindrical holes embedded in trenches." *Journal of Turbomachinery* 131, no. 1 (2009): 011003.

[13] Maikell, Jonathan, David Bogard, Justin Piggush, and Atul Kohli. "Experimental simulation of a film cooled turbine blade leading edge including thermal barrier coating effects." *Journal of Turbomachinery* 133, no. 1 (2011): 011014.

[14] Sundaram, N., and K. A. Thole. "Bump and trench modifications to film-cooling holes at the vane-endwall junction." *Journal of Turbomachinery* 130, no. 4 (2008): 041013.

[15] Lawson, Seth A., and Karen A. Thole. "Simulations of Multiphase Particle Deposition on Endwall Film-Cooling Holes in Transverse Trenches." *Journal of Turbomachinery* 134, no. 5 (2012): 051040.

[16] Stitzel, Sarah, and Karen A. Thole. "Flow field computations of combustor-turbine interactions relevant to a gas turbine engine." *J. Turbomach.* 126, no. 1 (2004): 122-129.

[17] Scrittore, Joseph. "Experimental study of the effect of dilution jets on film cooling flow in a gas turbine combustor." PhD diss., Virginia Tech, 2008.

[18] Vakil, Sachin Suresh, and Karen Ann Thole. "Flow and thermal field measurements in a combustor simulator relevant to a gas turbine aeroengine." *J. Eng. Gas Turbines Power* 127, no. 2 (2005): 257-267.